# Carotenogenesis Is Regulated by 5′UTR-Mediated Translation of Phytoene Synthase Splice Variants[1][OPEN]

**Daniel Álvarez, Björn Voß[2], Dirk Maass[3], Florian Wüst, Patrick Schaub, Peter Beyer, and Ralf Welsch***

Faculty of Biology, Institute for Biology II (D.A., D.M., F.W., P.S., P.B., R.W.), Institute for Biology III (B.V.), University of Freiburg, 79104 Freiburg, Germany

**ORCID IDs: 0000-0002-5930-2295 (D.A.); 0000-0002-9941-5550 (F.W.); 0000-0002-8529-4161 (P.S.); 0000-0002-2865-2743 (R.W.).**

Phytoene synthase (PSY) catalyzes the highly regulated, frequently rate-limiting synthesis of the first biosynthetically formed carotene. While *PSY* constitutes a small gene family in most plant taxa, the Brassicaceae, including Arabidopsis (*Arabidopsis thaliana*), predominantly possess a single *PSY* gene. This monogenic situation is compensated by the differential expression of two alternative splice variants (ASV), which differ in length and in the exon/intron retention of their 5′UTRs. ASV1 contains a long 5′UTR (untranslated region) and is involved in developmentally regulated carotenoid formation, such as during deetiolation. ASV2 contains a short 5′UTR and is preferentially induced when an immediate increase in the carotenoid pathway flux is required, such as under salt stress or upon sudden light intensity changes. We show that the long 5′UTR of ASV1 is capable of attenuating the translational activity in response to high carotenoid pathway fluxes. This function resides in a defined 5′UTR stretch with two predicted interconvertible RNA conformations, as known from riboswitches, which might act as a flux sensor. The translation-inhibitory structure is absent from the short 5′UTR of ASV2 allowing to bypass translational inhibition under conditions requiring rapidly increased pathway fluxes. The mechanism is not found in the rice (*Oryza sativa*) *PSY1* 5′UTR, consistent with the prevalence of transcriptional control mechanisms in taxa with multiple *PSY* genes. The translational control mechanism identified is interpreted in terms of flux adjustments needed in response to retrograde signals stemming from intermediates of the plastid-localized carotenoid biosynthesis pathway.

Carotenoids comprise a large group of plant-derived isoprenoids exerting numerous functions in plants. In chloroplast-containing tissues, they participate in photosynthesis, contribute to photoprotection, and provide biosynthetic precursors for the phytohormones abscisic acid (ABA) and strigolactones. Through biosynthetic processes, carotenoids are thus involved in developmental processes, response to abiotic stresses, mycorrhizal symbiosis, and the infestation by root parasitic weeds (Walter et al., 2010). Carotenoids also accumulate in chromoplasts to attract pollinating insects and to support zoochoric seed dispersal (Cazzonelli and Pogson, 2010; Li and Yuan, 2013).

The flux of carbon through the carotenoid biosynthetic pathway is frequently controlled by phytoene synthase (PSY). While its substrate geranylgeranyl diphosphate (GGPP) can enter through cyclization reactions and prenyl transfer onto nonprenyl acceptors into a variety of pathways (tocopherols, chlorophylls, plastoquinones, phylloquinones, and gibberellins; Beck et al., 2013; Ruiz-Sola et al., 2016), the head-to-head condensation of GGPP represents the first carotenoid-specific reaction. Phytoene desaturation and isomerization subsequently yield phytofluene, $\zeta$-carotene, and finally, the red-colored lycopene, which is cyclized, forming $\beta$- or $\varepsilon$-ionone endgroups. Subsequent hydroxylation and epoxidation reactions lead to the typical complement of plant xanthophylls. The synthesis of the two carotenoid-derived hormones, strigolactones and ABA, branches off from 9-cis-$\beta$-carotene and 9-cis-xanthophylls, respectively (Schwartz et al., 1997; Alder et al., 2012).

Because of the rate-limiting property, it is not surprising that *PSY* is highly regulated and that expression levels often correlate with the amounts of carotenoids or their derivatives formed. For instance, *PSY* is light regulated during photomorphogenesis and drives increased carotenoid biosynthesis during greening (von Lintig et al., 1997; Welsch et al., 2000, 2003; Rodríguez-Villalón et al., 2009). *PSY* is also induced during carotenoid accumulation in fruits and flowers (Schledz et al., 1996; Fraser et al., 1999; Qin et al., 2011). Moreover, induced *PSY* expression was shown to support ABA formation in roots (Li et al., 2008; Welsch et al., 2008; Ruiz-Sola et al., 2014). Accordingly, *PSY* overexpression is frequently sufficient to increase the carotenoid content in plants, including crops (Farré et al., 2010). For instance, increased

[1] This work was supported by the HarvestPlus research consortium.

[2] Present address: University of Stuttgart, Institute of Biochemical Engineering, Computational Biology, Stuttgart, Germany.

[3] Present address: Dentsply Friadent, Mannheim, Germany.

* Address correspondence to ralf.welsch@biologie.uni-freiburg.de.

The author responsible for distribution of materials integral to the findings presented in this article in accordance with the policy described in the Instructions for Authors (www.plantphysiol.org) is: Ralf Welsch (ralf.welsch@biologie.uni-freiburg.de).

R.W. and P.B. conceived this project and designed all experiments; D.A., D.M., B.V., and F.W. performed experiments and analyzed data; P.S. contributed new analytic tools; R.W. and P.B. wrote the article.

[OPEN] Articles can be viewed without a subscription.

www.plantphysiol.org/cgi/doi/10.1104/pp.16.01262

 

β-carotene levels were achieved in cassava roots, tomato fruit, carrot roots, and in nongreen tissues of Arabidopsis (*Arabidopsis thaliana*; Shewmaker et al., 1999; Paine et al., 2005; Fraser et al., 2007; Maass et al., 2009; Welsch et al., 2010).

However, PSY is also subjected to posttranscriptional control mechanisms. Bypassing transcriptional and translational processes, the membrane-association of soluble inactive PSY enzyme leads to rapid enzymatic activation (Welsch et al., 2000). Moreover, PSY protein levels were recently found to be posttranslationally regulated by the ORANGE proteins in Arabidopsis (Zhou et al., 2015). Additionally, potential feedback-regulatory mechanisms involve translation, plastid import, protein-protein interaction, and protein turnover to achieve stoichiometrically defined carotenoid biosynthetic complexes (Cazzonelli and Pogson, 2010; Nogueira et al., 2013; Arango et al., 2014; Avendaño-Vázquez et al., 2014; Tian, 2015).

This raises questions on how transcriptional and posttranscriptional mechanisms act in concert to meet the different tissue, developmental, and stress-related carotenoid requirements. Seemingly, in most taxa, there is a work-sharing as witnessed by the fact that *PSY* constitutes a small gene family of generally three members showing differential transcriptional regulation (Walter et al., 2015). In contrast, Arabidopsis and most other Brassicaceae have only one single *PSY* gene (Arabidopsis Genome Initiative, 2000). This suggests the coevolvement of special regulatory mechanisms to cope with the various physiological conditions that are not different from other plants. These mechanisms would be expected to act posttranscriptionally.

We show here that two splice variants are formed from the single *PSY* gene in Arabidopsis. They differ in the composition and length of their 5′UTRs and in their abundance in response to environmental cues. A pronounced translation-inhibitory function is mediated by the 5′UTR (untranslated region) of only the longer variant, which is not concluded for the 5′UTR of the short variant. The long 5′UTR version is capable of switching between translation-permissive and non-permissive states, a property that resides in a defined nucleotide stretch. This appears as a novel determinant of carotenoid biosynthesis that might relate to mechanisms reminiscent of riboswitches.

## RESULTS

### Two Differentially Regulated *AtPSY* Alternative Splice Variants with Different 5′UTRs

Two *AtPSY* alternative splice variants (ASVs) were identified in the TAIR database (https://www.arabidopsis.org). They differ in the length and in the exon/intron retention of their 5′UTR. Recent transcript start site analyses suggest that both splice variants emerge from different premRNAs through alternative transcription initiation (Morton et al., 2014; a scheme on the formation of both ASVs is shown in Fig. 1A; a sequence alignment is shown in Supplemental Fig. S1). The 5′UTR from ASV1 contains 403 nucleotides and is composed of two exons, which results from the complete elimination of intron 1 from the *AtPSY* premRNA variant 1. The second variant ASV2 was identified through EST analysis and retains a part of intron 1, but completely lacks exon 1 referring to premRNA 1, resulting in a truncated 5′UTR of only 252 nucleotides (Alexandrov et al., 2006). Using 5′UTR-specific primer/probe combinations, which allowed distinguishing between both ASVs, we investigated whether *AtPSY* ASVs respond differentially to light and upon salt stress, both parameters inducing *AtPSY* expression (von Lintig et al., 1997; Ruiz-Sola et al., 2014). We also used a primer/probe combination positioned within the *AtPSY* open reading frame (ORF) to equally capture both ASVs (Fig. 1A).

*AtPSY* induction during deetiolation relied almost completely on increased levels of ASV1, while ASV2 contributed only slightly within the first 2 h illumination but quickly returned to ground levels (Fig. 1B). Upon salt stress (200 mM NaCl), ASV1 reached a 2-fold level after 2 h, while ASV2 responded stronger attaining 4-fold induction (Fig. 1C). The effect of rapidly increased light intensity was tested with leaves from 4-week-old plants that were dark-adapted for 2 h and illuminated with white light for 4 h (Fig. 1D). A 4-fold induction of the ASV2 was found, while ASV1 was largely unresponsive. This correlated with a strong increase in PSY protein levels and with strongly increased AtPSY enzyme activity (Fig. 1, E and F). PSY activity was tested in the presence of norflurazon, which inhibits phytoene desaturation, resulting in the accumulation of phytoene (Beisel et al., 2010; Lätari et al., 2015). This revealed that phytoene synthesis was completely stalled during dark adaptation but became active upon illumination, concomitant with increased ASV2 expression and AtPSY protein levels. Concluded from the qRT-PCR results, transcripts from ASV1 were more abundant than those of ASV2 in all tissues analyzed. For instance, the difference was 20-fold in roots and 5-fold in illuminated leaves, but 140-fold in etiolated seedlings, which agrees with the contribution of ASV2 induction in these tissues (Fig. 1G). These results suggest that immediate biosynthetic requirements caused by environmental cues rely on ASV2, while ASV1 might rather contribute to those arising during developmental processes, such as deetiolation.

### The Structure of *PSY* 5′UTRs Determines Translation Effectiveness

A phylogenetic analysis with *PSY* 5′UTRs from various taxa revealed that Arabidopsis *PSY* 5′UTRs were closer related with those of other Brassicaceae (Fig. 2A). In contrast, non-Brassicaceae *PSY* 5′UTRs were on separate branches and showed a less-structured clade pattern. This suggests the presence of a functional feature in Brassicaceae 5′UTRs causing the conservation that is absent from 5′UTRs of other taxa. In fact, in silico

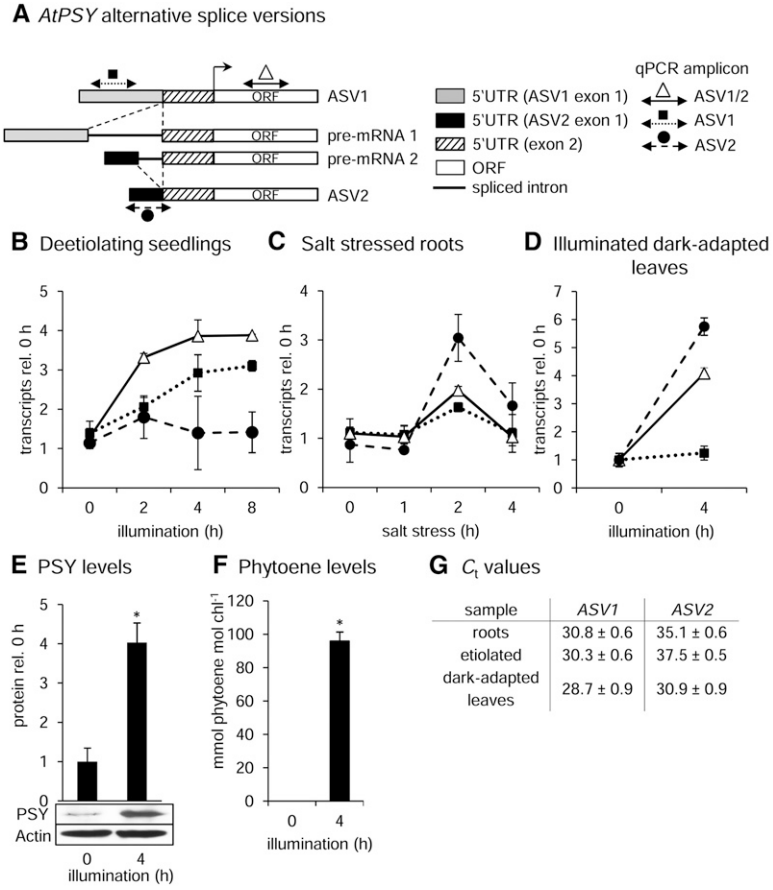


| sample | ASV1 | ASV2 |
|---|---|---|
| roots | 30.8 ± 0.6 | 35.1 ± 0.6 |
| etiolated | 30.3 ± 0.6 | 37.5 ± 0.5 |
| dark-adapted leaves | 28.7 ± 0.9 | 30.9 ± 0.9 |

**Figure 1.** Selective expression of alternative *AtPSY* variants. Transcript levels of two *AtPSY* ASVs with different 5′UTRs were investigated by qRT-PCR in Arabidopsis wild type. A scheme on different exon/intron retentions and the positions of amplicons used to discriminate both variants is shown in A (ASV1: 403 nucleotides, black square/dotted line; ASV2: 252 nucleotides, black circle/dashed line). Both ASVs were captured by amplification within the *AtPSY* ORF (ASV1/2: white triangle/solid line). Transcript levels in deetiolating seedlings (B), in roots of hydroponically grown seedlings transferred to medium containing 200 mM NaCl (C) and in leaves dark-adapted for 2 h and upon illumination with white light for 4 h (D). E, PSY protein levels and F, phytoene levels indicating PSY activity, determined by HPLC in illuminated dark-adapted leaves, incubated with norflurazon. G, Cycle threshold ($C_t$) values ± SD of ASV1 and ASV2 from samples with comparable *18S* rRNA levels. Normalized transcript levels were expressed relative to levels prior to illumination or salt treatment, respectively; results are the average ± SD of three biological replicates; *significant difference to the wild type (Student's *t* test, $P < 0.05$).

RNA analyses revealed a structural consensus with the Brassicaceae *PSY* 5′UTR sequences exclusively with the long 5′UTR from *AtPSY* (ASV1). These structural features were completely lost when the short 5′UTR of *AtPSY* (ASV2) or when non-Brassicaceae *PSY* 5′UTRs were included. The consensus structure for seven Brassicaceae *PSY* 5′UTRs is shown in Figure 2A and reveals one multiloop followed by a hairpin loop at the 5′ moiety (the structure at higher resolution and the structure-annotated alignment are shown in Supplemental Figs. S2 and S3).

This structural conservation of the 5′UTR of *AtPSY* (ASV1) led us to perform a functional analysis. For this, we overexpressed in Arabidopsis the full-length 5′UTR as well as 5′ truncations, all fused with the *AtPSY* open reading frame (ORF) under control of the *35S* promoter (*35Spro*). In order to disrupt structural elements, one truncation to 330 nucleotides affected the 5′ multiloops, and one further truncation, leaving 280 nucleotides, affected the hairpin structure in addition. Moreover, we constitutively overexpressed the *AtPSY* ORF without its 5′UTR. Transgenic lines were selected by qRT-PCR (using primers amplifying within the *AtPSY* ORF), which showed a comparable range of transgene expression levels (Fig. 2B).

Immunoblot analyses revealed that AtPSY protein levels were not any higher as in wild-type leaves in lines overexpressing the full-length 5′UTR version of 403 nucleotides, just like the truncation to 330 nucleotides (Fig. 2B). In contrast, further truncation to 280 nucleotides allowed very high AtPSY protein levels to accumulate, which were similar to lines overexpressing the 5′UTR-free *AtPSY* ORF. In conclusion, the 5′UTR inhibits translation of the *AtPSY* ORF with a crucial contribution that may be associated with the structural integrity of the hairpin loop.

### *AtPSY* 5′UTR-Mediated Translational Inhibition Determines Carotenoid Levels in Nongreen Tissues

In leaves, carotenoids remain at wild-type levels despite increased AtPSY protein, as present in lines expressing *AtPSY* without a 5′UTR or when equipped with the translation-permissive truncation to 280 nucleotides (Supplemental Fig. S4). This compensation of flux increase is at least partially caused by CCD4-mediated carotenoid degradation leading to the formation of apocarotenoids (Lätari et al., 2015). In contrast, roots do respond with carotenoid accumulation upon flux increases (Maass et al., 2009; Welsch et al., 2010). Roots of lines expressing the *AtPSY* ORF containing translation-inhibitory 5′UTR versions (403 and 330 nucleotides) contained AtPSY protein levels as low as in the wild type remaining close to the detection limit

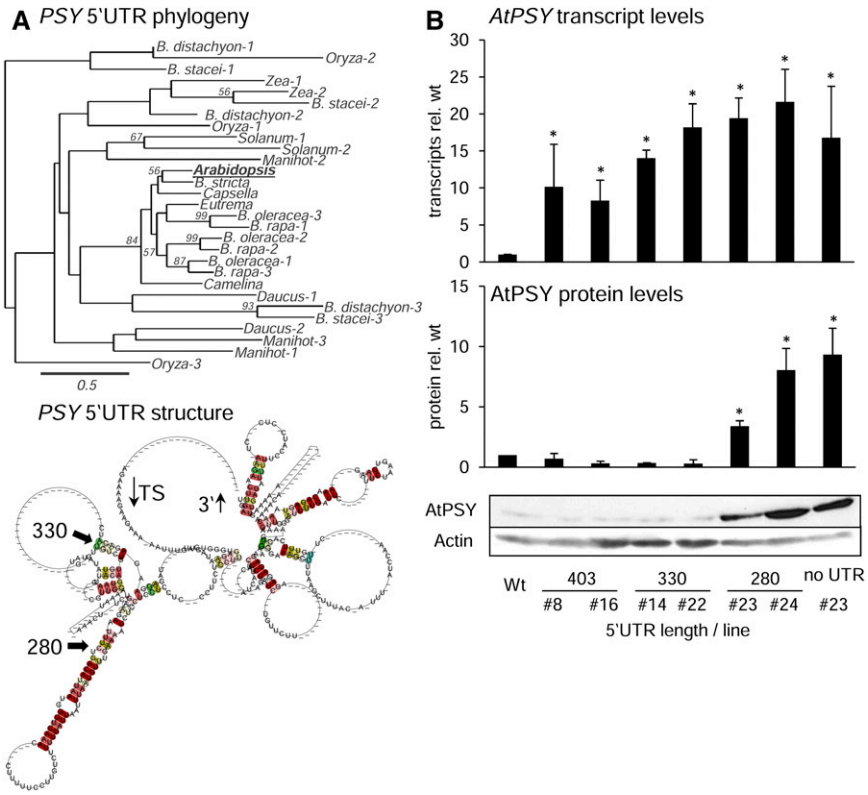


**Figure 2.** Sequence-dependent 5′UTR-mediated control of *AtPSY* ORF translation in Arabidopsis leaves. A, Phylogenetic tree generated from *PSY* 5′UTR sequences. The Arabidopsis *PSY* ASV1 5′UTR was used; for full taxa names and accession numbers, see Supplemental Table S2. Bootstrap values are reported next to the branches (only bootstraps above 50% are shown). A consensus structure of *PSY* 5′UTR predicted from Brassicaceae *PSY* 5′UTRs is shown below. Different colors indicate whether base pairs are formed by one (red), two (yellow), or three (green) different combinations of nucleotides; hyphens indicate gaps within the alignment. 5′UTR truncations used in B are indicated by arrows. TS, transcription start. B, Analyses of Arabidopsis leaves overexpressing the *AtPSY* ORF with full-length (403 nucleotides), 330 nucleotides, and 280 nucleotides of the 5′UTR of ASV1. *AtPSY* transcript (top) and AtPSY protein levels (bottom); actin-normalized protein levels relative to the wild type (Wt) are shown above. Data are the average ± SD of three biological replicates; *significant difference (Student's *t* test, $P < 0.05$).

(Fig. 3). Carotenoid levels were little, however significantly, elevated by 2- to 3-fold over the wild-type control. In contrast, the translation-permissive 280 nucleotides truncation allowed very high AtPSY protein levels accompanied by dramatically increased carotenoids reaching up to 40-fold of the wild-type levels. This is similar to lines overexpressing the *AtPSY* ORF lacking the *AtPSY* 5′UTR.

Nongreen callus derived from seedlings responded analogously (Maass et al., 2009, Supplemental Fig. S5). We took advantage of the visual carotenoid accumulation in response to high AtPSY protein levels to screen for orange calli with 90 additional transgenic events expressing *AtPSY* in conjunction with translation-inhibitory 5′UTR versions (*35Spro:5UTR403-AtPSY* and *35Spro:5UTR330-AtPSY* lines). However, we did not find any. This confirms that the presence of long *AtPSY* 5′UTRs inhibits translation and that the observed mechanism is independent of positional effects, i.e. transgene expression levels.

### Translational Inhibition Is Absent from the Poaceae *PSY1* 5′UTR

The structural dissimilarities between *PSY* 5′UTRs of Brassicaceae (mostly monogenic for *PSY*) and other taxa (with multiple *PSY* genes) led us to conclude that the 5′UTR-mediated translational inhibition might be absent from the latter. To test, we used rice (*Oryza sativa*) possessing three *PSY* paralogs. Rice *PSY1* (*OsPSY1*) transcripts are more abundant than *OsPSY2* in most tissues, while *OsPSY3* is stress responsive (Li et al., 2008; Welsch et al., 2008). Moreover, *OsPSY1* has the longest 5′UTR covering 275 nucleotides (*OsPSY2*: 56 nucleotides, *OsPSY3*: 226 nucleotides). Therefore, as in the previous experiments, the *OsPSY1* 5′UTR was combined with the *AtPSY* ORF and the chimeric transcript constitutively expressed in Arabidopsis followed by the analysis of roots and leaves (Fig. 4). In contrast to the findings with the *AtPSY* 5′UTR, the full-length *OsPSY1* 5′UTR did not inhibit translation; AtPSY protein was high in leaves and roots with strongly increased carotenoid levels detectable only in roots, as expected.

### Translation Inhibition in Vitro and Effect on Reporter Gene Expression

The translation-inhibitory function involving 123 nucleotides of the *AtPSY* 5′UTR was further investigated in vitro using wheat germ lysate and in vitro transcribed *AtPSY* 5′UTR/ORF versions. Equal amounts of RNA (see "Materials and Methods") were translated in the presence of [$^{35}$S]Met followed by SDS-PAGE and autoradiography. The incorporation into [$^{35}$S]AtPSY showed the same tendency as in planta, i.e. the lowest translation rates were observed with inhibitory 5′UTR versions (403 and 330 nucleotides), while further deletion of the 5′UTR to 280 nucleotides or its complete elimination almost doubled the translation efficiency (Fig. 5A).

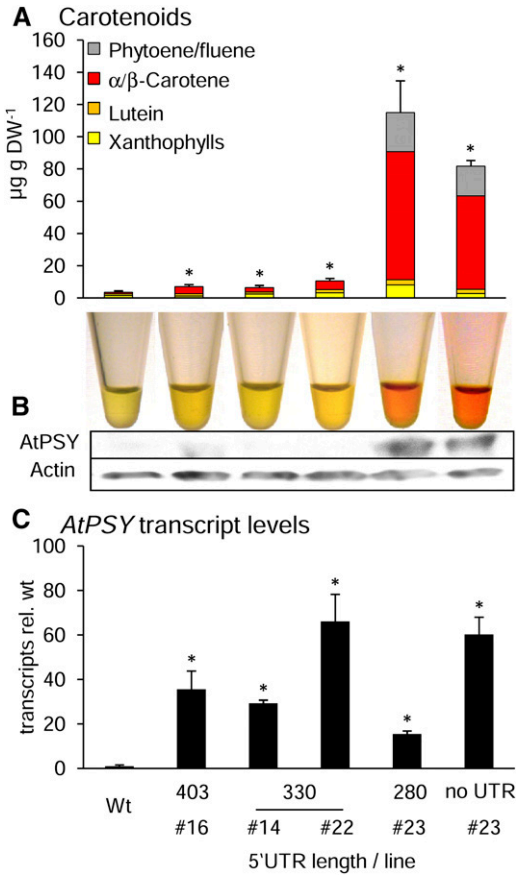


**Figure 3.** 5′UTR-regulated AtPSY translation efficiency determines carotenoid levels in roots. The *AtPSY* ORF with different lengths of the 5′UTR from ASV1 was overexpressed in Arabidopsis. Root carotenoid content (A) increased only in lines with only 280 nucleotides or no *AtPSY* 5′UTR. Chloroform extracts are shown below. AtPSY protein amounts are shown in (B) with actin as loading control. C, *AtPSY* transcript levels. Data are the average ± SD of three biological replicates; *significant difference to the wild type (Wt; Student's *t* test, $P < 0.05$).

To further generalize our findings, we placed the *AtPSY* 5′UTR and its truncations into a different context, namely upstream of *GUS*. Transgenic Arabidopsis lines expressing the *GUS* ORF lacking the *AtPSY* 5′UTR were included as a control. Expression was controlled by the *35Spro* as above. As GUS enzyme activity reflects well GUS protein levels (Koo et al., 2007), the translation efficiency was estimated by determining the ratio of GUS activity and *GUS* mRNA expression in leaves of three independent transgenic events each (Fig. 5B). Compared to the ratio determined for control lines without 5′UTR, lines overexpressing the translation-inhibitory 5′UTR versions (403 and 330 nucleotides) showed an up to 3-fold reduced ratio of GUS activity/transcript level. In contrast, lines overexpressing the translation-permissive 280-nucleotide *AtPSY* 5′UTR were similar to the control lines without *AtPSY* 5′UTR. These results indicate that the translation inhibition of the *AtPSY* 5′UTR functions independently of the ORF. However, the about 3-fold difference is contrasted by a larger, up to 10-fold difference achieved with AtPSY levels (Fig. 2B). This difference might be caused by feedback control mechanisms acting on protein levels (see "Discussion").

### Structural Analysis of *PSY* 5′UTRs

Our results suggest that the *AtPSY* 5′UTR negatively affects translation of the proximate ORF. Known examples for UTR-controlled translation initiation often involve regulatory RNA-binding proteins (Piccinelli and Samuelsson, 2007). However, a search for putative motifs of known RNA-binding regulatory proteins within the *AtPSY* 5′UTR using UTRscan (Grillo et al., 2010) revealed only two cis-acting elements prevailing in animal systems (Supplemental Table S1). Experiments were carried out to affinity-purify putative binding proteins from leaf cytoplasmic extracts using in vitro transcribed full-length *AtPSY* 5′UTR tagged with a streptomycin-binding RNA aptamer (Windbichler and Schroeder, 2006). However, the mass spectrometry-identified proteins were mostly

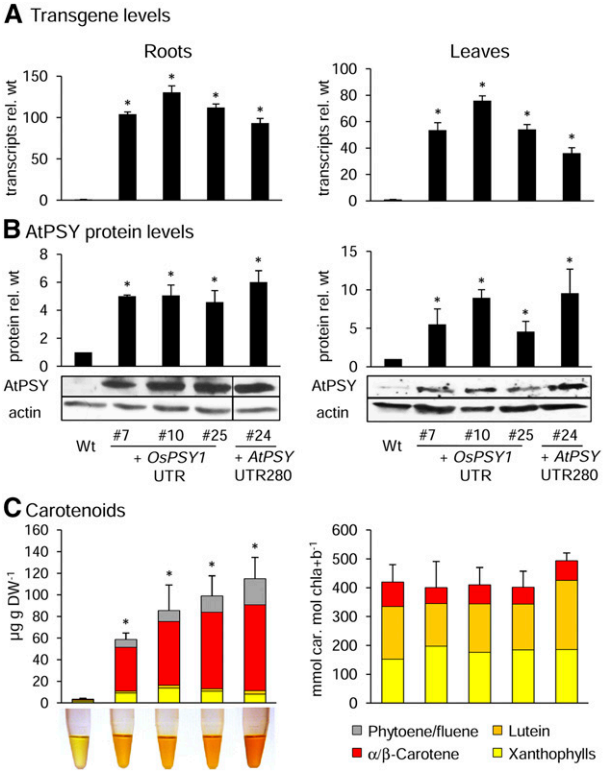


**Figure 4.** Rice *PSY1* 5′UTR has no translation inhibitory function in Arabidopsis. The *AtPSY* ORF containing the full-length rice *PSY1* 5′UTR (*OsPSY1 UTR*) was expressed in Arabidopsis. One line expressing the translation-permissive 280-nucleotide truncation of the *AtPSY* ASV1 5′UTR was included as a control (*AtPSY-UTR280*). Roots and leaves were analyzed for transgene transcript levels (A), AtPSY protein levels (B; actin-normalized AtPSY protein levels are shown above), and carotenoid levels, determined by HPLC (C). Root chloroform extracts are shown below. Data are the average ± SD of three biological replicates; *significant difference to wild type (wt; Student's *t* test, $P < 0.05$). DW, Dry weight.

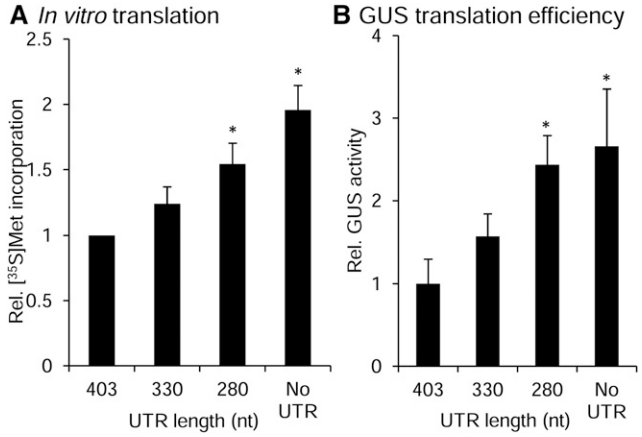


**Figure 5.** *AtPSY* 5′UTR translation inhibition in vitro and effect on *GUS* expression. A, In vitro translation. The *AtPSY* ORF with various lengths of its 5′UTR was in vitro transcribed and in vitro translated in wheat germ lysate in presence of [$^{35}$S]Met. Incorporation into [$^{35}$S]AtPSY was determined by SDS-PAGE followed by autoradiography and expressed relative to the [$^{35}$S]AtPSY amount obtained with the *5UTR403-AtPSY* mRNA version. Results are the average ± SEM of five biological replicates; *significant difference to *5UTR403-AtPSY* (Student's *t* test, $P < 0.05$). B, GUS translation efficiency. The *GUS* ORF with different lengths of the *AtPSY* 5′UTR was expressed in Arabidopsis. GUS enzyme activity was normalized to corresponding *GUS* transcript levels in leaves of 4-week-old plants and expressed relative to one reference line. Results are average ± SD of three biological replicates from three events per transformation; *significant difference to *5UTR403-GUS*-expressing line (Student's *t* test, $P < 0.05$).

not located in the cytoplasm or were not reproducibly enriched (Supplemental Data Set S1). The only RNA-binding protein detected was the Pumilio protein APUM5, a posttranscriptional repressor involved in virus defense binding at the 3′UTR of target transcripts (Huh et al., 2013). However, overexpression of *APUM5* as well as an *APUM5* RNAi line showed unchanged AtPSY protein levels compared to the wild type (Supplemental Fig. S6).

### Bioinformatic Analysis of *PSY* 5′UTRs

As indicated by the truncations, a feature determined by the 330- to 280-nucleotide stretch of the *AtPSY* 5′UTR governs the inhibitory function. Since no 5′UTR-binding proteins could be identified, we considered the possibility of protein-independent mechanisms involving structural RNA alterations induced by the binding of an effector, reminiscent to riboswitches. We used the conformational switch prediction program paRNAss (Giegerich et al., 1999; Voss et al., 2004) to investigate this possibility. For a given RNA sequence, paRNAss analyzes the folding space (the set of all possible secondary structures) within an energy range above the minimum free energy structure, calculates their pairwise distances via tree alignment and energy barriers, and plots these against each other. The folding space of an RNA switch is expected to harbor two clusters of structurally and kinetically related RNA structures that are clearly separated from each other. For each cluster, a consensus structure is derived and validated by comparison to the initial set of structures. A switch-like folding space is confirmed when two clouds of points are displayed—one near the x axis and one near the y axis.

These criteria apply for the inhibitory 403 nucleotides as well as the 330 nucleotides of *AtPSY* 5′UTR, as

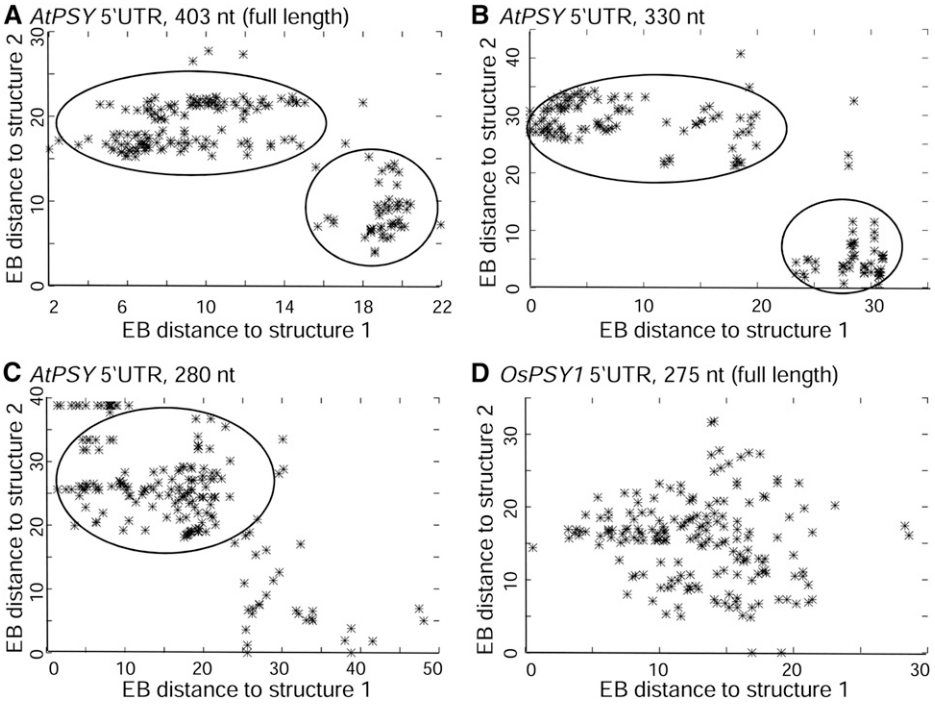


**Figure 6.** Conformational switch analysis of *AtPSY* and *OsPSY1* 5′UTRs. Energy barrier (EB in kcal mol$^{-1}$) distances of 5′UTR RNA secondary structures to respective consensus structures were predicted with paRNAss. Two clouds of energetically separable RNA structures are predicted for translation-inhibitory *AtPSY* 5′UTR versions (A, full length, 403 nucleotides; B, 330 nucleotides), while only one cloud is predicted for translation-permissive *AtPSY* 5′UTR truncation (C, 280 nucleotides). In contrast, distance calculations for the full-length *OsPSY1* 5′UTR spread over the diagram and do not form distinct clusters, which is in agreement with the absence of a translation-regulatory function (D).

shown in the consensus structure validation plots in Figure 6 (distance plots are provided in Supplemental Fig. S7). The plots confirm the presence of two energetically separable RNA structural populations, since two clouds appear. In consideration of the experimental data, one may interpret that one conformation confers translational inhibition while the switch into the second would result in a translation-permissive structure. The switch prediction for the noninhibitory 280-nucleotide *AtPSY* 5′UTR using identical parameters revealed only one cloud (Fig. 6C). Analogously, this truncation mediates only one preferred structural population and disallows the second structure (present in 403 and 330 nucleotides). Thus, the translation-permissive conformation might be permanently present in the 280-nucleotide version of the 5′UTR. The 50 nucleotides between 330 and 280 nucleotides are essential to switch into the inhibitory structure, which fits with the observations. As expected from the experimental results, a switch prediction for the full-length 5′UTR of *OsPSY1* failed, as indicated by the scattered spread of pairwise distance calculations over the diagram (Fig. 6D). Therefore, full-length *OsPSY1* and *AtPSY* 5′UTR differ strongly with respect to their structural as well as functional properties.

Intriguingly, the shorter 5′UTR present in the second *AtPSY* variant ASV2 eliminates the central hairpin loop fully and is therefore expected to exhibit a translation-permissive 5′UTR, similar to the 280-nucleotide truncation of the ASV1 5′UTR. Supporting this assumption, consensus structure validation of ASV2 5′UTR revealed one cloud, similar to the translation-permissive 280-nucleotide truncation of ASV1 (Supplemental Fig. S8).

### Carotenoid Pathway Flux Negatively Regulates Arabidopsis PSY Protein Levels

We have shown that the translation-inhibitory function of the full-length *AtPSY* 5′UTR is capable of coordinating AtPSY protein levels. Consequently, this transcription-independent mechanism has a strong impact on the activity of the whole biosynthetic pathway (see Fig. 3). This was demonstrated by monitoring AtPSY protein levels in Arabidopsis upon overexpression of the *AtPSY* ORF. However, it was impossible to discriminate between endogenous and ectopically expressed AtPSY in immunoblots. To be able to observe a potential feedback regulation acting on the protein levels of endogenous AtPSY in response to pathway activation, we generated transgenic lines expressing *35Spro:PSY1* versions from maize (*Zea mays*; *ZmPSY1*) and rice (*OsPSY1*). These pathway-activated lines were then analyzed using a monoclonal antibody that specifically recognizes Arabidopsis PSY. The line overexpressing *AtPSY* lacking its 5′UTR was included as control.

Transgene expression was first verified by qRT-PCR (Supplemental Fig. S9). Functional expression of Poaceae *PSY1* and *AtPSY* versions is witnessed by the efficient up-regulation of carotenogenesis in nongreen calli and roots, all attaining similar strongly increased carotenoid levels compared to the wild type (Fig. 7, A and B). As expected, leaf carotenoids were not much different, but an about 2-fold increased phytoene formation could be shown in all lines in vitro by using radioactive tracer experiments (Fig. 7, C and D; Supplemental Fig. S10).

The mRNA levels of both *AtPSY* ASVs were not much altered relative to the wild type in response to the increased pathway flux driven by *ZmPSY1* and *OsPSY1* expression (Fig. 7E). Unchanged endogenous *AtPSY* expression cannot explain the fact that the internal AtPSY protein was markedly reduced, reaching only 30% and 50% of wild-type levels in the *ZmPSY1* and *OsPSY1*-expressing lines, respectively (Fig. 7F). As expected, the *AtPSY*-overexpressing line showed strongly increased AtPSY protein levels with this antibody. It is therefore concluded that increased pathway activity yields a feedback signal capable of attenuating the translation of the internal *AtPSY* mRNA. Since this contains a population of the long ASV1 variant, this signal might consist of a pathway-derived metabolite capable of inducing structural RNA switching, similar to a riboswitch.

## DISCUSSION

### Compensation of the Single-Gene Situation by Alternative Transcription and Alternative Splicing

The genomic organization of *PSY* genes suggests that *PSY* orthologs evolved by gene multiplication accompanied by their functional diversification (Li et al., 2008; Welsch et al., 2008; Arango et al., 2010; Ampomah-Dwamena et al., 2015). The multigene situation often coincides with the development of chromoplasts, implying that additional *PSY* genes might be required for this purpose, as shown in tomato (*Solanum lycopersicum*), melons (*Cucumis melo*), yellow maize, and banana (*Musa* sp.; Fraser et al., 1994; Gallagher et al., 2004; Qin et al., 2011; Mlalazi et al., 2012). Conversely, several *PSY* paralogs are also present in taxa that do not develop chromoplasts, such as in rice and in white maize varieties. This suggests an advantage of maintaining multiple *PSY* genes to cope with chloroplast carotenoid metabolism (Gallagher et al., 2004; Li et al., 2009). In fact, pathway flux control though *PSY* is required, e.g. during abiotic stress for increased ABA formation (Li et al., 2008; Welsch et al., 2008; Arango et al., 2010), upon mycorrhization (Walter et al., 2015) and during deetiolation (von Lintig et al., 1997; Welsch et al., 2000; Rodríguez-Villalón et al., 2009).

The monogenic situation for *PSY* present in Arabidopsis and other Brassicaceae might be interpreted as the result of the overall genome size reduction in these species (Hu et al., 2011). The resulting loss of transcriptional versatility may have increased the pressure toward developing novel or harnessing existing posttranscriptional mechanisms of regulation. In line with this notion, two alternative splice variants differing in their 5′UTR derive from the single *PSY* gene in Arabidopsis and may

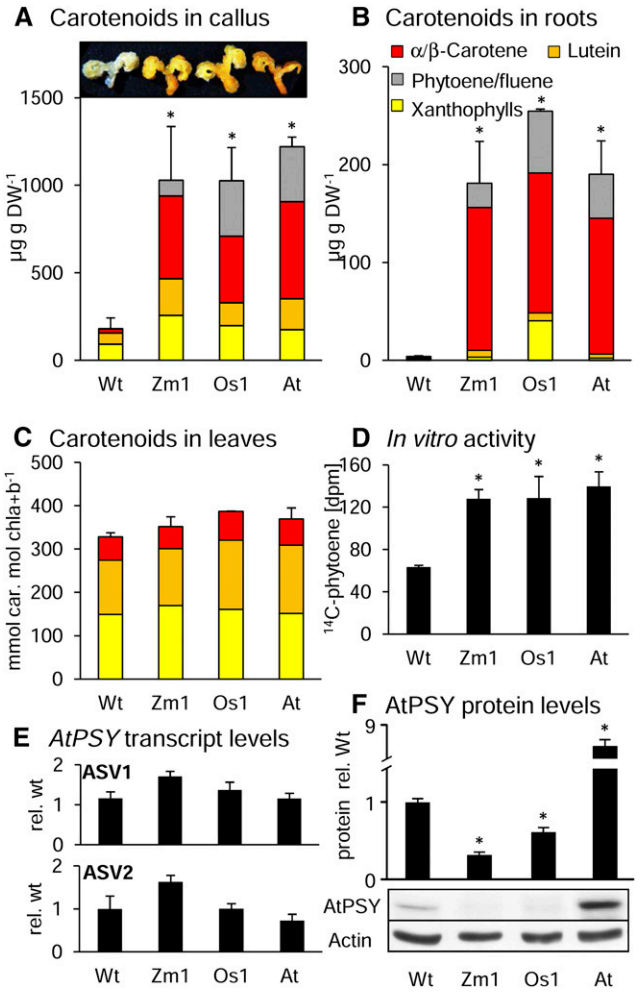


**Figure 7.** Carotenoid flux negatively regulates Arabidopsis PSY protein levels in leaves. *PSY* ORFs from maize (Zm), rice (Os), and Arabidopsis (At) were expressed in Arabidopsis. In seed-derived callus (A) and roots (B), this results in increased carotenoid levels compared to wild-type control (wt). Representative calli are shown above A. In contrast, in leaves, carotenoids were as in the wild type (C), although pathway flux was increased, as determined by in vitro PSY activity assays with isolated chloroplast membranes, incubated with DMAPP, [1-$^{14}$C]IPP, and GGPP synthase (D). In leaves, this did not affect transcript levels of both *AtPSY* ASVs determined by qRT-PCR (E) but down-regulated protein levels of endogenous AtPSY. An immunoblot using AtPSY-specific antibodies and actin as loading control is shown in F; quantification of normalized AtPSY protein levels relative to wild type is shown above. As expected, AtPSY levels are strongly increased in the *AtPSY*-overexpressing line. Data are average ± SD of three biological replicates. DW, dry weight; *significant difference to the wild type (Wt; Student's *t* test, $P < 0.05$).

represent a first level of downstream diversification to cope with reduced genetic information. Alternative splicing is known to respond to environmental stimuli, e.g. changes in light intensity or abiotic stresses (Staiger and Brown, 2013). In fact, both *AtPSY* splice variants differ in their expression patterns with ASV2 (short 5′UTR) predominating under salt and light stresses, while the expression of ASV1 (long 5′UTR) predominates during deetiolation; it might be specific for triggering carotenogenesis in developmental programs (Fig. 1).

### Translational Control Exerted by the 5′UTR

Apparently, a second level of downstream regulatory diversification is implemented by translational control exerted by the long 5′UTRs present in ASV1. Here, a critical hairpin loop must be impaired to warrant high translation rates while the short 5′UTR of ASV2, lacking this structure, is translation-permissive. This is witnessed by the fact that constructs containing the 5′UTR of ASV1 yielded AtPSY protein levels as low as in the wild type, independent of expression levels. Truncations of the 5′UTR showed that a 330-nucleotide 5′UTR maintained the inhibitory function, while further truncation to 280 nucleotides led to high protein levels like in lines overexpressing the *AtPSY* ORF. Accordingly, structural changes occurring upon truncation to 280 nucleotides fosters translation. Moreover, our bioinformatic analyses suggest that the 330- to 280-nucleotide region is critical to maintain an RNA structure capable of switching between two defined conformations. This raises the need for a factor or factors capable of inducing the switching function, a hallmark of riboswitches, and suggests a switchable change between translation-inhibitory and translation-permissive states (Manzourolajdad and Arnold, 2015).

This function is evident when looking at tissue-specific differences. In wild-type roots, AtPSY protein levels were close to detection limit, but we could easily detect AtPSY in wild-type leaves, suggesting that AtPSY protein levels are higher in leaves than in roots (compare Figs. 3B and 4B with Figs. 1E and 7F). Remarkably, these quantitative differences are reproduced in leaves and roots of lines expressing the inhibitory *AtPSY* 5′UTR versions, while the expression of the *AtPSY* ORF alone yields high levels in both tissues. This indicates that the *AtPSY* 5′UTR coordinates the translation efficiency of the *AtPSY* ORF according to tissue-specific carotenoid requirements, which are very different in leaves compared with roots.

The mechanisms by which translational control is exerted can only be a matter of speculation at this point. All 5′UTR/*AtPSY* ORF combinations were expressed under control of the *35Spro*, and thus, 5′capped transcripts will form. Accordingly, a comparable capacity to recruit ribosomal subunits to initiate ribosome scanning can be assumed. However, secondary structures within 5′UTRs are known to affect ribosome scanning and thus translation efficiency, suggesting that this might be impeded by the structures formed by the full-length *AtPSY* 5′UTR (Fraser, 2015).

### Functional Diversification versus Translational Control

In contrast to the *AtPSY* 5′UTR of ASV1 the *PSY1* 5′UTR from rice (containing three paralogs) is not translation inhibitory. The absence of interconvertible structures in the *OsPSY1* 5′UTR also predicts the

absence of a regulatory switch function, which is in agreement with our data.

This indicates that equivalent translational mechanisms are either absent in rice or not functional in an Arabidopsis background. However, it is conceivable that the need for translational control is diminished when flux control can be realized by means of differential expression from multiple *PSY* loci. Interestingly, there are exceptions in the Brassicaceae, like cabbage (*Brassica rapa*) and cauliflower (*Brassica oleraceae*), where three *PSY* paralogs prevail. They show functional redundancy with signs of subfunctionalization among green and nongreen tissues (Cárdenas et al., 2012; López-Emparán et al., 2014; Li et al., 2015). Although the 5′UTRs of these *PSYs* show sequence homology with the long translation-inhibitory *AtPSY* 5′UTR of ASV1, they are more distant (Fig. 2A). This may reflect a later reestablishment of multiple *PSYs* that occurred after primary reduction as suggested for these species (Cárdenas et al., 2012). They might be viewed as being "en route" toward the reestablishment of a functional differentiation through *PSY* gene multiplication.

### Flux-Dependent Translational Control of PSY Mediated by the 5′UTR

Our data show that increased pathway activity, as achieved by the expression of Poaceae *PSY1* genes, down-regulates the protein levels of the internal AtPSY without affecting its expression (Fig. 7). Since no interacting protein factors could be identified—in fact, 5′UTR-binding proteins controlling cytoplasmic translation are barely known from plants—the possibility of a low molecular mass compound capable of inducing the structural change of the 5′UTR needs to be considered.

In wild-type leaves, considerable amounts of carotenoids are constantly synthesized but also consumed by photo-oxidative processes, forming carotenoid cleavage products, some of which are volatile (Simkin et al., 2003; Ramel et al., 2013). Upon pathway flux increase, such as in lines with higher PSY protein levels, steady-state carotenoid levels are maintained. This is only partially explained by increased CCD4-mediated cleavage into apocarotenoids (Lätari et al., 2015). This indicates that there are additional mechanisms capable of compensating flux overflow; the feedback control of carotenoid synthesis would represent the most sustainable solution. In nongreen tissues, the relevance of feedback-controlled AtPSY translation may be in the prevention of carotenoid accumulation in the form of microcrystals, which are thought to be largely inaccessible by CCDs and thus exempt from homeostatic control (Maass et al., 2009; Nogueira et al., 2013).

Because of enzymatic and nonenzymatic carotenoid turnover, flux-dependent regulation of AtPSY translation calls for the involvement of a signaling molecule originating directly or indirectly from carotenoids. Carotenoids per se are too lipophilic to be transported out of the plastid. However, short-chained apocarotenoids formed through carotenoid cleavage by nonenzymatic as well as enzymatic processes, and derivatives thereof are more water-soluble and have been shown to act as signaling metabolites, capable of relaying plastid-derived information into other compartments, to bind to receptors and induce downstream events (Tian, 2015; Hou et al., 2016). Prominent examples are ABA and strigolactones, involved in stress response and shoot-branching control, respectively, the signaling pathways of which are well understood. Since ABA levels were unchanged in response to *PSY1* expression in leaves (Supplemental Fig. S11), its involvement in the post-transcriptional down-regulation of AtPSY appears unlikely. However, additional, hitherto unidentified carotenoid-derived metabolites with signaling function have been reported as being involved in the feedback regulation of carotenogenic gene expression (Diretto et al., 2006; Bai et al., 2009; Kachanovsky et al., 2012; Galpaz et al., 2013) and in the control of developmental processes (Avendaño-Vázquez et al., 2014; Van Norman et al., 2014; Tian, 2015). Furthermore, altered carotenoid patterns, achieved by overexpressing a downstream carotene hydroxylase, reduced PSY protein amounts in cultivated carrots by a posttranscriptional mechanism (Arango et al., 2014).

An apocarotenoid derivative acting as a signal for the plastid carotenoid state might bind to the 5′UTR to initiate the riboswitch-like mechanism discussed above. Although a cytokinin-responsive riboswitch was suggested recently (Grojean and Downes, 2010), the thiamine pyrophosphate (TPP) riboswitch is the only confirmed case in plants thus far (Sudarsan et al., 2003; Bocobza and Aharoni, 2014). However, the TPP riboswitch is clearly distinct from the mechanism controlling AtPSY translation—it involves alternative intron splicing upon TPP-induced 3′UTR structural changes,

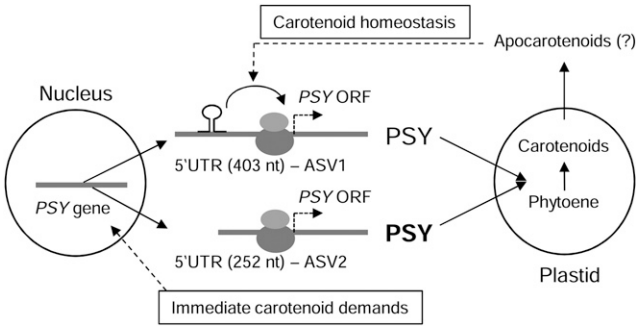


**Figure 8.** Model for the posttranscriptional regulation of PSY in Arabidopsis. Regulation of PSY protein amount entails two translational control elements realized by ASVs differing in their 5′UTR length. ASV1 contains 403-nucleotide 5′UTR, which coordinates translation with the carotenoid pathway flux and is suggested to be regulated by plastid-derived apocarotenoids. Translation inhibition requires a hairpin loop the elimination of which results in a translation-permissive 5′UTR. This structural element is absent in the 252-nucleotide 5′UTR of ASV2, which therefore bypasses feedback-regulated translational control and is able to quickly increase PSY protein levels, e.g. for higher carotenoid consumption by photo-oxidation in illuminated leaves or for ABA biosynthesis in salt-stressed roots.

which destabilizes mRNA resulting in reduced protein amounts (Thore et al., 2006; Wachter et al., 2007). Thus, more work is needed to substantiate the involvement of metabolite-driven conformational changes in the *AtPSY* 5′UTR in the posttranscriptional regulation of the carotenoid pathway flux.

It appears unlikely that changes in mRNA stability, which can depend on sequence elements within 5′UTR, are involved (Hansen et al., 2001; Bhat et al., 2004). This is because the effects of the 5′UTR on AtPSY protein levels were clearly independent from transgene mRNA levels. Other potential 5′UTR-located translational control mechanisms include peptides translated from noncanonical start ATGs interacting with pathway intermediates (Roy and von Arnim, 2013) or interfering with the downstream translation of the canonical ORF (upstream ORF [uORF]). An uORF is, in fact, present at position 265 in the *AtPSY* 5′UTR. However, it is thus included in all truncations analyzed and can therefore not be relevant.

We have shown that the translation-based attenuation of carotenoid pathway flux is also apparent when the long 5′UTR is fused to *GUS* as an alternative ORF. However, the effect was less pronounced, as compared to the results obtained with the *AtPSY* ORF. In an interpretation, this is caused by reduced feedback control: While *PSY* expression will always promote pathway activity, this is not the case with GUS. Consequently, the presumed signaling metabolites will not be formed at elevated levels so that a feedback response reflecting the steady-state wild-type situation will only be observed.

In summary, the down-regulation of endogenous AtPSY in lines expressing Poaceae *PSY1* can be interpreted as an effort to restrict the perceived increase in pathway flux. This suggests a cross-talk between carotenoid levels and translation efficiency that employs the 5′UTR as a "sensor," capable of undergoing a transition into a translation-permissive configuration. This interpretation of our data is summarized in a model shown in Figure 8.

## MATERIALS AND METHODS

### Generation of Transgenic Arabidopsis Lines and Growth Conditions

The vector backbone for all constructs including the *AtPSY* ORF was *pCAMBIA1390-35Spro*, which was cloned as described (Welsch et al., 2007). For *pC1390-35:5UTR403-AtPSY*, the *AtPSY* ORF (Maass et al., 2009) was fused with its full-length 5′UTR obtained from a genomic clone containing the *PSY* gene (Welsch et al., 2003) by overlap extension PCR and subcloned into *pCAMBIA1390-35Spro*. ORFs containing truncated 5′UTR versions were obtained by PCR amplification using mutagenized primers and subcloning. Similarly, the ORFs from *ZmPSY1* (Paine et al., 2005) and *OsPSY1* (Welsch et al., 2008) were amplified by PCR and subcloned into *pCAMBIA-35Spro*. The 5′UTR of *OsPSY1* was amplified from reverse-transcribed leaf total RNA, fused with the *AtPSY* ORF by overlap extension PCR, and subcloned into *pCAMBIA1390-35S*. The vector *pC1390-35S::GUSPlus* was used to express *AtPSY* 5′UTR with *GUS* as reporter gene. The full-length *AtPSY* 5′UTR of ASV1 and truncations were amplified by PCR from the binary plasmids described above and subcloned between the *35Spro* and the *GUS* gene. Arabidopsis (*Arabidopsis thaliana*; ecotype Wassilewskija) was transformed by vacuum infiltration (Bechtold and Pelletier, 1998). Homozygous T2 progenies were identified by the segregation pattern of the corresponding T3 progenies on Murashige and Skoog plates containing hygromycin (30 $\mu$g mL$^{-1}$). Arabidopsis lines overexpressing the *AtPSY* ORF were as in Maass et al. (2009).

Arabidopsis was grown with 100 $\mu$mol photons m$^{-2}$ s$^{-1}$ under long-day conditions. For illumination of dark-adapted leaves, leaves from 4-week-old plants were incubated in water for 2 h in the dark, followed by illumination with 200 $\mu$mol m$^{-2}$ s$^{-1}$ for 4 h. Norflurazon treatments and hydroponic cultures were performed as described (Lätari et al., 2015). For salt-stress experiments, seedlings were transferred to medium containing 200 mM NaCl.

### Carotenoid and ABA Analysis

Rosette leaves from 4-week-old plants grown on soil were used. Roots were retrieved from plants grown hydroponically (Hétu et al., 2005). Seed-derived callus were generated according to Maass et al. (2009). Carotenoids were extracted from lyophilized tissues (leaves: 5 mg; roots: 100 mg; callus: 30 mg) with acetone and quantified by HPLC as described (Welsch et al., 2008). ABA extraction was performed as described (Welsch et al., 2008).

### qRT-PCR

Total RNA was isolated using the plant RNA purification reagent (Invitrogen); DNAseI digestion and cleanup was performed with Zymoprep (Zymo Research). qRT-PCR assays were performed as described (Welsch et al., 2008). Sequences of primers and 6FAM-labeled TaqMan probes are given in Supplemental Table S3. Gene expression levels were normalized to *18S* rRNA, detected using the eukaryotic *18S* rRNA endogenous control kit (Life Technologies).

### In Vitro Phytoene Synthase Activity

Plastid isolation from leaves of 4-week-old Arabidopsis plants was performed according to Welsch et al. (2000). Pellets were resuspended in 2 mL of lysis buffer (20 mM Tris, pH 8.0, and 4 mM $MgCl_2$) and incubated on ice for 10 min; membranes were pelleted by centrifugation at 21,000*g* for 10 min, resuspended in 300 mL of assay buffer (100 mM Tris/HCl, pH 7.6, 20% [v/v] glycerol, 2 mM $MnCl_2$, 10 mM $MgCl_2$, and 1 mM 3,3′,3′′-phosphanetriyltripropanoic acid); and protein concentration was determined using the Bio-Rad Protein Assay. For in vitro phytoene synthesis, 200 $\mu$g protein was incubated with 10 $\mu$M [1-$^{14}$C]-isopentenyl diphosphate (IPP; 50 mCi mmol$^{-1}$; American Radiolabeled Chemicals), 20 $\mu$M IPP (isoprenoids.com), 40 $\mu$M dimethylallyl diphosphate, 4 mM ATP, and 10 $\mu$g of recombinant, purified geranylgeranyl diphosphate synthase (Kloer et al., 2006) for 15 min. Product analysis and quantification was performed by scintillation counting and thin-layer chromatography scanning as described (Welsch et al., 2000). Data represent the mean ± SD of two sampling times each from two biological replicates.

### Quantitative GUS assay

GUS activity was determined as described by Jefferson et al. (1987). For GUS protein extraction, 100 mg of tissue were ground with 1 mL of extraction buffer (50 mM $Na_2HPO_4/H_3PO_4$, pH 7.0, 1 mM EDTA, 0.1% [w/v] *N*-laurylsarcosine, 0.1% [v/v] Triton X-100, and 10 mM $\beta$-mercaptoethanol). After centrifugation (14,000*g*, 15 min, 4°C), 5 $\mu$L supernatant was mixed with 395 $\mu$L of 0.56 mM methylumbelliferyl-$\beta$-D-glucuronide in extraction buffer and incubated at 37°C. Four aliquots of 300 $\mu$L were collected every 15 min, and the reactions were stopped with 0.3 M $Na_2CO_3$. Fluorescence analysis was made in duplicate with 200 $\mu$L sample volume in a POLARStar Omega (BMG Labtech) microplate reader (excitation: 365 nm; emission: 445 nm) and 4-methylumbelliferone concentrations calculated from a standard regression curve. Protein concentration of supernatants was determined by Bradford assay (Bio-Rad), and GUS enzyme activity was expressed as pmol 4-methylumbelliferone min$^{-1}$ $\mu$g protein$^{-1}$.

### Bioinformatic Analysis

Conformational switch predictions were performed with paRNAss (Voss et al., 2004) on local optimal structures within 3 kcal mol$^{-1}$ above the minimum free energy structure. Local optimality of an individual structure was checked by reapplying the folding algorithm using this structure as a folding constraint and comparing the resulting structure with the initial one. If differences occurred, a neighboring structure (one base pair more or less) achieves a better

free energy. In this case, the initial structure was not locally optimal and therefore discarded. This step makes it possible to let paRNAss pick 100 structures without losing significance due to undersampling. paRNAss was applied using the tree alignment distance for structure comparison. Consensus structure analysis was performed with RNAalifold (Bernhart et al., 2008) with multiple sequence alignments performed with MAFFT v7 (http://mafft.cbrc.jp/alignment/server/). For the phylogenetic analysis, alignment was conducted with MUSCLE (Edgar, 2004), maximum likelihood phylogenetic reconstruction was carried out in PhyML v3.0 and bootstrap test was selected with 500 replicates (Guindon et al., 2005). Accession numbers of 5′UTR sequences used are given in Supplemental Table S2.

## In Vitro Transcription/Translation Assays

The *AtPSY* ORF was subcloned into the vector pGEM4, downstream of the *SP6* promotor. Versions carrying 5′UTR truncations were subcloned from the corresponding binary constructs. In vitro transcription was performed with 20 $\mu$g *Sal*I-linearized plasmids using the SP6-RiboMAX kit (Promega) in a reaction volume of 50 $\mu$L at 37°C for 4 h in the presence of 0.25 $\mu$Ci [8-$^{14}$C]ATP (57.9 mCi mmol$^{-1}$, 0.05 mCi ml$^{-1}$; GE Healthcare). DNAseI digestion and RNA cleanup was performed using Qiagen RNeasy columns. RNA integrity was checked on formaldehyde gels.

In vitro translation was performed in wheat germ lysate (Promega), supplemented with 2.5 $\mu$L 1 M potassium acetate and 1 $\mu$g mRNA at 25°C. Equimolar amounts of mRNA species were calculated after the determination of [8-$^{14}$C]ATP incorporation by scintillation counting (Tri-Carb2900TR; Perkin-Elmer).

Translation assays were performed in 50 $\mu$L in the presence of 25 $\mu$Ci of [$^{35}$S]met (Redivue ProMix, 1.2 Ci mmol$^{-1}$, 10 mCi ml$^{-1}$; GE Healthcare). For comparative translation efficiency measurements, 5 $\mu$L aliquots were removed within the linear phase (15 min), 20 $\mu$L 3× SDS sample buffer was added, subjected to SDS-PAGE, transferred to PVDF membranes, and autoradiographed using a Phosphor-Imager screen (Fuji Film). Quantification of [$^{35}$S]AtPSY radioactivity was performed with the Quantity One software (Bio-Rad). Data were expressed relative to the [$^{35}$S]AtPSY amounts detected in the *5UTR403-AtPSY* sample of the first measuring time point. The data represent the mean ± SD of three independent in vitro translations from independently transcribed mRNAs.

## Immunoblot Analyses

Proteins were extracted with phenol as described (Maass et al., 2009). A hybridoma cell line producing monoclonal antibodies against AtPSY was obtained from Abmart, antibodies were purified (BioSS Toolbox) and used in a final concentration of 12 $\mu$g mL$^{-1}$. Immunoblots were developed with Pierce ECL western blotting substrate (Thermo Scientific). After deactivation of bound peroxidase (Sennepin et al., 2009), imunoblots were reprobed with antiactin antibodies (Sigma-Aldrich). Signal quantification was done using ImageJ (Abramoff et al., 2004).

## Accession Numbers

Sequence data from this article can be found in the EMBL/GenBank data libraries under accession numbers NM_001161243 (*AtPSY* premRNA variant 1, At5g17230.1), DR368718.1 (*AtPSY* premRNA variant 2, At5g17230.2), U32636 (*ZmPSY1*), and NM_001065182 (*OsPSY1*). Accession numbers for annotations in the phylogenetic tree in Figure 2A are given in Supplemental Table S2.

## Supplemental Data

The following supplemental materials are available.

**Supplemental Figure S1.** Comparison of *AtPSY* 5′UTRs from two alternative splice variants.

**Supplemental Figure S2.** Consensus structure of full-length *PSY* 5′UTR.

**Supplemental Figure S3.** Structure-annotated alignment of *PSY* 5′UTR sequences.

**Supplemental Figure S4.** Carotenoid levels in *AtPSY*-overexpressing lines.

**Supplemental Figure S5.** 5′UTR regulated PSY translation efficiency determines carotenoid levels in callus.

**Supplemental Figure S6.** AtPSY in Arabidopsis lines with altered APUM5 levels.

**Supplemental Figure S7.** Conformational switch analyses of *AtPSY* and *OsPSY1* 5′UTRs.

**Supplemental Figure S8.** Conformational switch analysis of *AtPSY* 5′UTR splice variant 2.

**Supplemental Figure S9.** Transgene and *AtPSY* ORF expression in *PSY*-overexpressing Arabidopsis lines.

**Supplemental Figure S10.** $^{14}$C-labeled compounds formed in an in vitro PSY activity assay.

**Supplemental Figure S11.** Relative ABA content of *PSY*-overexpressing Arabidopsis lines.

**Supplemental Table S1.** cis-acting elements in *AtPSY* 5′UTR predicted by UTRScan.

**Supplemental Table S2.** Accession numbers of *PSY* 5′UTR sequences used.

**Supplemental Table S3.** Primers and probes used for qRT-PCR.

**Supplemental Data Set S1.** Proteins identified from 5′UTR affinity-purified cytoplasmic extracts.

## ACKNOWLEDGMENTS

We thank Daniel Lang and Wolfgang R. Hess (University of Freiburg) for valuable discussions. We also thank Kyung-Hee Peak (Korea University) for supplying seeds from *APUM5*-overexpressing and RNAi lines and Pavel Salavei (BioSS Toolbox, Freiburg) for his excellent work in monoclonal antibody purification, Ana Paula Sanchez Carranza for her help with RNA extraction, and Carmen Schubert (University of Freiburg) for skillful technical assistance.

Received August 25, 2016; accepted October 5, 2016; published October 11, 2016.

## LITERATURE CITED

**Abramoff MD, Magelhaes PJ, Ram SJ** (2004) Image Processing with ImageJ. Biophotonics Int. **11:** 36–42

**Alder A, Jamil M, Marzorati M, Bruno M, Vermathen M, Bigler P, Ghisla S, Bouwmeester H, Beyer P, Al-Babili S** (2012) The path from $\beta$-carotene to carlactone, a strigolactone-like plant hormone. Science **335:** 1348–1351

**Alexandrov NN, Troukhan ME, Brover VV, Tatarinova T, Flavell RB, Feldmann KA** (2006) Features of Arabidopsis genes and genome discovered using full-length cDNAs. Plant Mol Biol **60:** 69–85

**Ampomah-Dwamena C, Driedonks N, Lewis D, Shumskaya M, Chen X, Wurtzel ET, Espley RV, Allan AC** (2015) The Phytoene synthase gene family of apple (*Malus x domestica*) and its role in controlling fruit carotenoid content. BMC Plant Biol **15:** 185

**Arabidopsis Genome Initiative** (2000) Analysis of the genome sequence of the flowering plant *Arabidopsis thaliana.* Nature **408:** 796–815

**Arango J, Jourdan M, Geoffriau E, Beyer P, Welsch R** (2014) Carotene hydroxylase activity determines the levels of both $\alpha$-carotene and total carotenoids in orange carrots. Plant Cell **26:** 2223–2233

**Arango J, Wüst F, Beyer P, Welsch R** (2010) Characterization of phytoene synthases from cassava and their involvement in abiotic stress-mediated responses. Planta **232:** 1251–1262

**Avendaño-Vázquez A-O, Cordoba E, Llamas E, San Román C, Nisar N, De la Torre S, Ramos-Vega M, Gutiérrez-Nava MD, Cazzonelli CI, Pogson BJ, et al** (2014) An uncharacterized apocarotenoid-derived signal generated in $\zeta$-carotene desaturase mutants regulates leaf development and the expression of chloroplast and nuclear genes in Arabidopsis. Plant Cell **26:** 2524–2537

**Bai L, Kim E-H, DellaPenna D, Brutnell TP** (2009) Novel lycopene epsilon cyclase activities in maize revealed through perturbation of carotenoid biosynthesis. Plant J **59:** 588–599

**Bechtold N, Pelletier G** (1998) *In planta Agrobacterium*-mediated transformation of adult *Arabidopsis thaliana* plants by vacuum infiltration. Methods Mol Biol **82:** 259–266

**Beck G, Coman D, Herren E, Ruiz-Sola MA, Rodríguez-Concepción M, Gruissem W, Vranová E** (2013) Characterization of the GGPP synthase gene family in *Arabidopsis thaliana*. Plant Mol Biol **82:** 393–416

**Beisel KG, Jahnke S, Hofmann D, Köppchen S, Schurr U, Matsubara S** (2010) Continuous turnover of carotenes and chlorophyll a in mature leaves of Arabidopsis revealed by 14CO2 pulse-chase labeling. Plant Physiol **152:** 2188–2199

**Bernhart SH, Hofacker IL, Will S, Gruber AR, Stadler PF** (2008) RNAalifold: improved consensus structure prediction for RNA alignments. BMC Bioinformatics **9:** 474

**Bhat S, Tang L, Krueger AD, Smith CL, Ford SR, Dickey LF, Petracek ME** (2004) The Fed-1 (CAUU)4 element is a 5′ UTR dark-responsive mRNA instability element that functions independently of dark-induced polyribosome dissociation. Plant Mol Biol **56:** 761–773

**Bocobza SE, Aharoni A** (2014) Small molecules that interact with RNA: riboswitch-based gene control and its involvement in metabolic regulation in plants and algae. Plant J **79:** 693–703

**Cárdenas PD, Gajardo HA, Huebert T, Parkin IA, Iniguez-Luy FL, Federico ML** (2012) Retention of triplicated phytoene synthase (PSY) genes in *Brassica napus* L. and its diploid progenitors during the evolution of the Brassiceae. Theor Appl Genet **124:** 1215–1228

**Cazzonelli CI, Pogson BJ** (2010) Source to sink: regulation of carotenoid biosynthesis in plants. Trends Plant Sci **15:** 266–274

**Diretto G, Tavazza R, Welsch R, Pizzichini D, Mourgues F, Papacchioli V, Beyer P, Giuliano G** (2006) Metabolic engineering of potato tuber carotenoids through tuber-specific silencing of lycopene epsilon cyclase. BMC Plant Biol **6:** 13

**Edgar RC** (2004) MUSCLE: multiple sequence alignment with high accuracy and high throughput. Nucleic Acids Res **32:** 1792–1797

**Farré G, Sanahuja G, Naqvi S, Bai C, Capell T, Zhu C, Christou P** (2010) Travel advice on the road to carotenoids in plants. Plant Sci **179:** 28–48

**Fraser CS** (2015) Quantitative studies of mRNA recruitment to the eukaryotic ribosome. Biochimie **114:** 58–71

**Fraser PD, Enfissi EMA, Halket JM, Truesdale MR, Yu D, Gerrish C, Bramley PM** (2007) Manipulation of phytoene levels in tomato fruit: effects on isoprenoids, plastids, and intermediary metabolism. Plant Cell **19:** 3194–3211

**Fraser PD, Kiano JW, Truesdale MR, Schuch W, Bramley PM** (1999) Phytoene synthase-2 enzyme activity in tomato does not contribute to carotenoid synthesis in ripening fruit. Plant Mol Biol **40:** 687–698

**Fraser PD, Truesdale MR, Bird CR, Schuch W, Bramley PM** (1994) Carotenoid biosynthesis during tomato fruit development (evidence for tissue-specific gene expression). Plant Physiol **105:** 405–413

**Gallagher CE, Matthews PD, Li F, Wurtzel ET** (2004) Gene duplication in the carotenoid biosynthetic pathway preceded evolution of the grasses. Plant Physiol **135:** 1776–1783

**Galpaz N, Burger Y, Lavee T, Tzuri G, Sherman A, Melamed T, Eshed R, Meir A, Portnoy V, Bar E, et al** (2013) Genetic and chemical characterization of an EMS induced mutation in Cucumis melo *CRTISO* gene. Arch Biochem Biophys **539:** 117–125

**Giegerich R, Haase D, Rehmsmeier M** (1999) Prediction and visualization of structural switches in RNA. Pac Symp Biocomput **4:** 126–137

**Grillo G, Turi A, Licciulli F, Mignone F, Liuni S, Banfi S, Gennarino VA, Horner DS, Pavesi G, Picardi E, et al** (2010) UTRdb and UTRsite (RELEASE 2010): a collection of sequences and regulatory motifs of the untranslated regions of eukaryotic mRNAs. Nucleic Acids Res **38:** D75–D80

**Grojean J, Downes B** (2010) Riboswitches as hormone receptors: hypothetical cytokinin-binding riboswitches in *Arabidopsis thaliana*. Biol Direct **5:** 60

**Guindon S, Lethiec F, Duroux P, Gascuel O** (2005) PHYML Online—a web server for fast maximum likelihood-based phylogenetic inference. Nucleic Acids Res **33:** W557–W559

**Hansen ER, Petracek ME, Dickey LF, Thompson WF** (2001) The 5′ end of the pea ferredoxin-1 mRNA mediates rapid and reversible light-directed changes in translation in tobacco. Plant Physiol **125:** 770–778

**Hétu M-F, Tremblay LJ, Lefebvre DD** (2005) High root biomass production in anchored Arabidopsis plants grown in axenic sucrose supplemented liquid culture. Biotechniques **39:** 345–349

**Hou X, Rivers J, León P, McQuinn RP, Pogson BJ** (2016) Synthesis and function of apocarotenoid signals in plants. Trends Plant Sci **21:** 792–803

**Hu TT, Pattyn P, Bakker EG, Cao J, Cheng J-F, Clark RM, Fahlgren N, Fawcett JA, Grimwood J, Gundlach H, et al** (2011) The *Arabidopsis lyrata* genome sequence and the basis of rapid genome size change. Nat Genet **43:** 476–481

**Huh SU, Kim MJ, Paek K-H** (2013) Arabidopsis Pumilio protein APUM5 suppresses Cucumber mosaic virus infection via direct binding of viral RNAs. Proc Natl Acad Sci USA **110:** 779–784

**Jefferson RA, Kavanagh TA, Bevan MW** (1987) GUS fusions: beta-glucuronidase as a sensitive and versatile gene fusion marker in higher plants. EMBO J **6:** 3901–3907

**Kachanovsky DE, Filler S, Isaacson T, Hirschberg J** (2012) Epistasis in tomato color mutations involves regulation of phytoene synthase 1 expression by *cis*-carotenoids. Proc Natl Acad Sci USA **109:** 19021–19026

**Kloer DP, Welsch R, Beyer P, Schulz GE** (2006) Structure and reaction geometry of geranylgeranyl diphosphate synthase from *Sinapis alba*. Biochemistry **45:** 15197–15204

**Koo J, Kim Y, Kim J, Yeom M, Lee IC, Nam HG** (2007) A GUS/luciferase fusion reporter for plant gene trapping and for assay of promoter activity with luciferin-dependent control of the reporter protein stability. Plant Cell Physiol **48:** 1121–1131

**Lätari K, Wüst F, Hübner M, Schaub P, Beisel KG, Matsubara S, Beyer P, Welsch R** (2015) Tissue-specific apocarotenoid glycosylation contributes to carotenoid homeostasis in Arabidopsis leaves. Plant Physiol **168:** 1550–1562

**Li F, Tsfadia O, Wurtzel ET** (2009) The phytoene synthase gene family in the Grasses: subfunctionalization provides tissue-specific control of carotenogenesis. Plant Signal Behav **4:** 208–211

**Li F, Vallabhaneni R, Wurtzel ET** (2008) *PSY3*, a new member of the phytoene synthase gene family conserved in the *Poaceae* and regulator of abiotic stress-induced root carotenogenesis. Plant Physiol **146:** 1333–1345

**Li L, Yuan H** (2013) Chromoplast biogenesis and carotenoid accumulation. Arch Biochem Biophys **539:** 102–109

**Li P, Zhang S, Zhang S, Li F, Zhang H, Cheng F, Wu J, Wang X, Sun R** (2015) Carotenoid biosynthetic genes in *Brassica rapa*: comparative genomic analysis, phylogenetic analysis, and expression profiling. BMC Genomics **16:** 492

**López-Emparán A, Quezada-Martinez D, Zúñiga-Bustos M, Cifuentes V, Iñiguez-Luy F, Federico ML** (2014) Functional analysis of the *Brassica napus* L. phytoene synthase (PSY) gene family. PLoS One **9:** e114878

**Maass D, Arango J, Wüst F, Beyer P, Welsch R** (2009) Carotenoid crystal formation in Arabidopsis and carrot roots caused by increased phytoene synthase protein levels. PLoS One **4:** e6373

**Manzourolajdad A, Arnold J** (2015) Secondary structural entropy in RNA switch (Riboswitch) identification. BMC Bioinformatics **16:** 133

**Mlalazi B, Welsch R, Namanya P, Khanna H, Geijskes RJ, Harrison MD, Harding R, Dale JL, Bateson M** (2012) Isolation and functional characterisation of banana phytoene synthase genes as potential cisgenes. Planta **236:** 1585–1598

**Morton T, Petricka J, Corcoran DL, Li S, Winter CM, Carda A, Benfey PN, Ohler U, Megraw M** (2014) Paired-end analysis of transcription start sites in Arabidopsis reveals plant-specific promoter signatures. Plant Cell **26:** 2746–2760

**Nogueira, M, Mora, L, Enfissi, EMA, Bramley, PM Fraser, PD** (2013). Subchromoplast sequestration of carotenoids affects regulatory mechanisms in tomato lines expressing different carotenoid gene combinations. Plant Cell **25:** 4560–4579

**Paine JA, Shipton CA, Chaggar S, Howells RM, Kennedy MJ, Vernon G, Wright SY, Hinchliffe E, Adams JL, Silverstone AL, et al** (2005) Improving the nutritional value of Golden Rice through increased provitamin A content. Nat Biotechnol **23:** 482–487

**Piccinelli P, Samuelsson T** (2007) Evolution of the iron-responsive element. RNA **13:** 952–966

**Qin X, Coku A, Inoue K, Tian L** (2011) Expression, subcellular localization, and *cis*-regulatory structure of duplicated phytoene synthase genes in melon (*Cucumis melo* L.). Planta **234:** 737–748

**Ramel F, Mialoundama AS, Havaux M** (2013) Nonenzymic carotenoid oxidation and photooxidative stress signalling in plants. J Exp Bot **64:** 799–805

**Rodríguez-Villalón A, Gas E, Rodríguez-Concepción M** (2009) Phytoene synthase activity controls the biosynthesis of carotenoids and the supply of their metabolic precursors in dark-grown Arabidopsis seedlings. Plant J **60:** 424–435

**Roy B, von Arnim AG** (2013) Translational regulation of cytoplasmic mRNAs. Arabidopsis Book **11:** e0165

**Ruiz-Sola MÁ, Arbona V, Gómez-Cadenas A, Rodríguez-Concepción M, Rodríguez-Villalón A** (2014) A root specific induction of carotenoid biosynthesis contributes to ABA production upon salt stress in arabidopsis. PLoS One **9:** e90765

**Ruiz-Sola MÁ, Coman D, Beck G, Barja MV, Colinas M, Graf A, Welsch R, Rütimann P, Bühlmann P, Bigler L, et al** (2016) Arabidopsis GERANYLGERANYL DIPHOSPHATE SYNTHASE 11 is a hub isozyme required for the production of most photosynthesis-related isoprenoids. New Phytol **209:** 252–264

**Schledz M, al-Babili S, von Lintig J, Haubruck H, Rabbani S, Kleinig H, Beyer P** (1996) Phytoene synthase from *Narcissus pseudonarcissus*: functional expression, galactolipid requirement, topological distribution in chromoplasts and induction during flowering. Plant J **10:** 781–792

**Schwartz SH, Tan BC, Gage DA, Zeevaart JA, McCarty DR** (1997) Specific oxidative cleavage of carotenoids by VP14 of maize. Science **276:** 1872–1874

**Sennepin AD, Charpentier S, Normand T, Sarré C, Legrand A, Mollet LM** (2009) Multiple reprobing of Western blots after inactivation of peroxidase activity by its substrate, hydrogen peroxide. Anal Biochem **393:** 129–131

**Shewmaker CK, Sheehy JA, Daley M, Colburn S, Ke DY** (1999) Seed-specific overexpression of phytoene synthase: increase in carotenoids and other metabolic effects. Plant J **20:** 401–412

**Simkin AJ, Zhu C, Kuntz M, Sandmann G** (2003) Light-dark regulation of carotenoid biosynthesis in pepper (*Capsicum annuum*) leaves. J Plant Physiol **160:** 439–443

**Staiger D, Brown JWS** (2013) Alternative splicing at the intersection of biological timing, development, and stress responses. Plant Cell **25:** 3640–3656

**Sudarsan N, Barrick JE, Breaker RR** (2003) Metabolite-binding RNA domains are present in the genes of eukaryotes. RNA **9:** 644–647

**Thore S, Leibundgut M, Ban N** (2006) Structure of the eukaryotic thiamine pyrophosphate riboswitch with its regulatory ligand. Science **312:** 1208–1211

**Tian L** (2015) Recent advances in understanding carotenoid-derived signaling molecules in regulating plant growth and development. Front Plant Sci **6:** 790

**Van Norman JM, Zhang J, Cazzonelli CI, Pogson BJ, Harrison PJ, Bugg TDH, Chan KX, Thompson AJ, Benfey PN** (2014) Periodic root branching in Arabidopsis requires synthesis of an uncharacterized carotenoid derivative. Proc Natl Acad Sci USA **111:** E1300–E1309

**von Lintig J, Welsch R, Bonk M, Giuliano G, Batschauer A, Kleinig H** (1997) Light-dependent regulation of carotenoid biosynthesis occurs at the level of phytoene synthase expression and is mediated by phytochrome in *Sinapis alba* and *Arabidopsis thaliana* seedlings. Plant J **12:** 625–634

**Voss B, Meyer C, Giegerich R** (2004) Evaluating the predictability of conformational switching in RNA. Bioinformatics **20:** 1573–1582

**Wachter A, Tunc-Ozdemir M, Grove BC, Green PJ, Shintani DK, Breaker RR** (2007) Riboswitch control of gene expression in plants by splicing and alternative 3′ end processing of mRNAs. Plant Cell **19:** 3437–3450

**Walter MH, Floss DS, Strack D** (2010) Apocarotenoids: hormones, mycorrhizal metabolites and aroma volatiles. Planta **232:** 1–17

**Walter MH, Stauder R, Tissier A** (2015) Evolution of root-specific carotenoid precursor pathways for apocarotenoid signal biogenesis. Plant Sci **233:** 1–10

**Welsch R, Arango J, Bär C, Salazar B, Al-Babili S, Beltrán J, Chavarriaga P, Ceballos H, Tohme J, Beyer P** (2010) Provitamin A accumulation in cassava (*Manihot esculenta*) roots driven by a single nucleotide polymorphism in a phytoene synthase gene. Plant Cell **22:** 3348–3356

**Welsch R, Beyer P, Hugueney P, Kleinig H, von Lintig J** (2000) Regulation and activation of phytoene synthase, a key enzyme in carotenoid biosynthesis, during photomorphogenesis. Planta **211:** 846–854

**Welsch R, Maass D, Voegel T, Dellapenna D, Beyer P** (2007) Transcription factor RAP2.2 and its interacting partner SINAT2: stable elements in the carotenogenesis of Arabidopsis leaves. Plant Physiol **145:** 1073–1085

**Welsch R, Medina J, Giuliano G, Beyer P, Von Lintig J** (2003) Structural and functional characterization of the phytoene synthase promoter from *Arabidopsis thaliana*. Planta **216:** 523–534

**Welsch R, Wüst F, Bär C, Al-Babili S, Beyer P** (2008) A third phytoene synthase is devoted to abiotic stress-induced abscisic acid formation in rice and defines functional diversification of phytoene synthase genes. Plant Physiol **147:** 367–380

**Windbichler N, Schroeder R** (2006) Isolation of specific RNA-binding proteins using the streptomycin-binding RNA aptamer. Nat Protoc **1:** 637–640

**Zhou X, Welsch R, Yang Y, Álvarez D, Riediger M, Yuan H, Fish T, Liu J, Thannhauser TW, Li L** (2015) Arabidopsis OR proteins are the major posttranscriptional regulators of phytoene synthase in controlling carotenoid biosynthesis. Proc Natl Acad Sci USA **112:** 3558–3563